EURASIP Journal on Advances in Signal Processing

RESEARCH Open Access

IOT security privacy protection mechanism and mechanical structure design simulation optimization

Caiping Guo[1] and Daqing Li[2*]

* Correspondence: daqli@haue.edu.cn
[2]School of Mechanical Engineering, Henan Institute of Engineering, Zhengzhou 451191, Henan, China
Full list of author information is available at the end of the article

Abstract

Once the Internet of Things was proposed, it has received great attention from all walks of life and has become one of the top ten technologies that change the world. Therefore, more and more people are engaged in the research of the Internet of Things, after the unremitting efforts of all seniors. Now the Internet of Things has been applied to every aspect of our lives. However, in the application process of the Internet of Things, the protection of personal privacy will undoubtedly be involved. If this problem is not effectively resolved, it will become a major obstacle to the development of the Internet of Things. At present, the research of fully homomorphic technology has attracted great attention from the cryptography community. You can directly calculate the encrypted text encryption to obtain the output and decrypt the output. The result is the same as the output of the unencrypted plain text. This article first comprehensively describes the solution to the privacy protection problem in the existing Internet of Things, and then proposes to apply the fully homomorphic technology to the Internet of Things to make the services provided by the network more secure. Through the analysis of the basic composition and architecture of the existing Internet of Things system, a privacy protection interaction model for the Internet of Things is established, which uses a completely homomorphic technology. On this basis, the algorithm for implementing simple homomorphic encryption is improved, and general homomorphic encryption theory is proposed for some security issues. After using this method to encrypt privacy, the success rate of cracking dropped by 24%.

Keywords: Internet of Things, Security and privacy protection mechanism, Mechanical structure simulation and optimization, Fully homomorphic technology

1 Introduction

1.1 Background and Significance

Today, "Internet of Things" has become a new generation of popular technology concepts [1]. The International Telecommunication Union published a report entitled "Internet of Things." The report describes the beautiful scene of the Internet age: if the driver makes a mistake while driving, the car alarm system will automatically remind; the owner will have the file when he leaves. The bag will remind you what to bring;

the washing machine can read the signs of the clothes and automatically adjust to the appropriate water temperature requirements [2, 3]. In 1999, China proposed the concept of the Internet of Things, which was then called a sensor network. Its definition is according to the agreed agreement, use infrared sensors, and radio frequency identification (laser scanner, global positioning system, and other information tracking equipment) to connect to the Internet to achieve the purpose of information exchange and communication and intelligent identification, placement, tracking, and monitoring the purpose of management and management [4]. The network concept based on the "Internet concept" expands end users into goals and objects through the "Internet of Things Thought," and the goals and objects promote information exchange [5].

The emergence of the Internet of Things not only greatly facilitates our daily lives, but also has a huge impact on our society. And because of the importance attached to the Internet of Things all over the world, the development of the Internet of Things is also advancing rapidly [6, 7]. This paper focuses on the security and privacy protection mechanism of the Internet of Things in the simulation and optimization of mechanical structures [8, 9] and discusses the successful implementation of this method.

1.2 Related work

Due to the importance of the Internet of Things in today's society, more and more research teams have shifted their focus to the Internet of Things and achieved remarkable results. Khanouche predicted the application of the Internet of Things in actual scenarios through social development [10]. Although it was as expected in most directions, it did not refer to the development factors of the Internet of Things due to external environmental factors. In some parts of the prediction, there were errors [11]; Hodges analyzed the Internet of Things through the past development history [12]. However, the development speed of the Internet of Things is getting faster and faster, and it is obviously inappropriate to predict the future development of the Internet of Things through the previous development speed [13]. These methods are well-founded in some respects, but from an overall analysis, they appear narrow. Therefore, this article attempts to use the application of the Internet of Things to optimize the mechanical structure simulation and optimize the mechanical structure through simulation [14, 15].

1.3 Main content

This paper firstly uses 3D Solidwork modeling software to complete the establishment of the intelligent operator model, then introduces the built-in mechanical dynamics model into the ADAMS (Automatic Dynamic Analysis of Mechanical System) software for simulation, and finally uses the desktop software to complete the system simulation (structure optimization) [16, 17]. This article has the following innovations: (1) this article uses mechanical kinematics to study the movement of machinery, through which it can better analyze the mechanical movement process and optimize the machinery [18], and (2) this paper optimizes the mechanical motion through the inverse solution of the Motoman hp6 machine kinematics, which improves the optimization to a degree [2, 19].

2 Methods

2.1 Research methods of mechanical kinematics

The kinematics of the machine is to solve the stop (position and stop) at any point at the end of the machine when the parameters of each link of the machine are known. Active kinematics is very important in course design and machine trajectory control [20]. Figure 1 shows the solution flow of positive kinematics solution, and the transformation matrix of the final coupled coordinate system of the serial N-degree-of-freedom robot relative to the basic coordinate system can be calculated as follows:

$$ {}^{0}_{x}A = {}^{0}_{1}A{}^{1}_{2}A---{}^{X-2}_{X-1}A{}^{X-1}_{X}A \tag{1} $$

The position of ${}^{n}k = [k_a, k_b, k_c]$ any point that the robot ultimately links to the basic coordinates can be described as follows:

$$ {}^{0}k = {}^{0}_{1}A{}^{1}_{2}A---{}^{x-2}_{x-1}A{}^{x-1}_{x}Ak \tag{2} $$

The poses of any point on the robot ${}^{m}k = [k_a, k_b, k_c]$ links the coordinate system, and in another link, the coordinate system j (j<i) can be described as follows:

$$ yk = {}_{y+1}yA{}^{y+1}_{y+2}A\ldots{}^{z-1}_{z-2}A{}^{z-1}_{z}Azk \tag{3} $$

Introduce the D–H parameters of the connection coordinate system corresponding to the Motoman hp6 robot in Fig. 1, define the coordinate D_O system as the basic coordinate system, and define the uniform transformation of the final robot reference point D_6 coordinate system relative to the basic coordinate system:

$$ {}^{0}_{6}D = {}^{0}_{1}D{}^{1}_{2}D{}^{2}_{3}D{}^{3}_{4}D{}^{4}_{5}D{}^{5}_{6}D\begin{bmatrix} m_o & e_o & d_o & f_o \\ m_p & e_p & d_p & f_p \\ m_q & e_q & d_q & f_q \\ 0 & 0 & 0 & 0 \end{bmatrix} \tag{4} $$

2.2 Research method of inverse kinematics of Motoman Hp6 machine

The inverse trigonometric function is usually used to solve the angle problem to solve the inverse problem of robot kinematics. Using the bidirectional modulator function is a good way to solve this problem [21, 22]. The signs of and b can determine the quadrant where the arctangent 2 (a, b) is located, thereby determining the value of z.

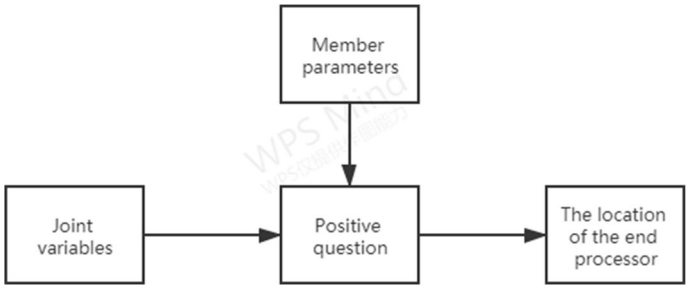

Fig. 1 Kinematics positive solution process

In the process of solving the inverse solution, in order to facilitate the insertion of xS + yC = z of the unary equation into the calculation, S and C represent the sine and cosine of the angle z, respectively. When after

$$z = \arctan2\left(z, \pm\sqrt{x^2 + y^2 - z^2}\right) - \arctan2(y, x) \tag{5}$$

According to the parameters of the robot connection coordinate system and the D-H parameters, a general 6R motion robot can be described as follows:

$${}^{0}_{6}D = \begin{bmatrix} m_o & e_o & d_o & f_o \\ m_p & e_p & d_p & f_p \\ m_q & e_q & d_q & f_q \\ 0 & 0 & 0 & 1 \end{bmatrix} \tag{6}$$

After deformation, we can get:

$${}^{2}_{3}D^{-1}\,{}^{1}_{2}D^{-1}\,{}^{0}_{1}D^{-1}\,{}^{0}_{6}D = {}^{3}_{4}D\,{}^{4}_{5}D\,{}^{5}_{6}D \tag{7}$$

The conversion of the left and right matrices is too complicated to be solved manually, so the Maple mathematics software with powerful computing capabilities is used to solve the two sides separately [23].

At the same time, the left matrix of the above type is declared as C(x,y). The matrix on the right is D(x,y). Solve the turning angle z:

Let C(1,2)=D(1,2), get:

$$-\sin z_1 k_a + \cos z_1 k_b = 0 \tag{8}$$

If $k_a = s\cos\alpha$, $k_b = s\sin\alpha$, the substitution can get:

$$\alpha_1 = \arctan2(k_a, k_b) \tag{9}$$

Solve angle $\alpha_1 and \alpha_2$

$$\begin{bmatrix} \cos\alpha_{23}\left(\cos\alpha_1 k_x + \sin\alpha_1 k_y - z_1\right) - \cos\alpha_{23} k_x - a_1 = \cos\alpha_3 k_2 \\ -\sin\alpha_{23}\left(\cos\alpha_1 k_x + \sin\alpha_1 k_y - z_1\right) - \cos\alpha_{23} k_x - a_1 = -\sin\alpha_3 k_2 \end{bmatrix} \tag{10}$$

After finishing:

$$\sin\alpha_{23}(b_5 k_z + k_4) + \cos\alpha_{23}(b_4 k_z + k_3) = \left(b_5{}^2 - k_z{}^2 - b_4{}^2 - k_3{}^2\right)/2 \tag{11}$$

2.3 Research methods of security and privacy

Lightweight cryptography is usually designed for hardware-oriented applications, so hardware implementation efficiency is an important part of performance evaluation [24]. Generally, a variety of different technical indicators (such as power consumption, maximum frequency, clock period, and circuit area) can be used to measure the efficiency of hardware implementation [25, 26]. Among them, energy consumption includes static energy consumption and dynamic energy consumption. The static power consumption is proportional to the circuit area. The larger the area, the higher the energy consumption; dynamic energy consumption is proportional to frequency and higher the frequency, the higher the power consumption. In order to meet the limits of power consumption in resource-limited environments (such as RFID (radio frequency identification) and wireless sensors), low-frequency clocks of 100 to 500kHz are usually

used [27]. Since the chip area is cost-effective to meet the cost requirements of resource-constrained areas (such as RFID), the best way is to try to reduce the circuit area requirements of the algorithm [28]. Therefore, the hardware performance of optical cryptography can be measured by the circuit area, and the circuit area of the algorithm can usually be measured by the number of equivalent gateway circuits [29], independent of its manufacturing technology. In the evaluation, we can request the number of GE (General Electric) required making general logic components from the standard cell library. These numbers are determined by digital circuits and design techniques, usually using standard 0.18-mm ASIC (Application Specific Integrated Circuit) libraries. In the hardware implementation of the algorithm, in addition to the resources occupied by various logical operations, the data storage in the intermediate process is also quite resource-consuming. For example, storing 1 bit requires 6-12GE, so storing the intermediate value of 128 bits requires at least 768GE.

And we know that the hardware implementation of lightweight cryptographic algorithms usually requires control to be around 2000GE (because the RFID storage capacity is only about 2000GE), so the storage capacity accounts for almost half of the total number of GE, so the lightweight cryptographic design reduces storage requirements. Generally, choosing a shorter packet length and key length and reducing repeated structure forwarding can effectively reduce the number of GE [30]. For example, when designing lightweight block encryption, the use of 64-bit block length can change from 128-bit block size. The length is reduced by at least 384 GE, and the length of an 80-bit key can save at least 288 GE compared to the length of a 128-bit GE key. In addition, the S-box is a basic unit that requires a relatively large amount of GE, and as the S-box increases, the number of GE required geometrically increases. For example, the commonly used 44×S-box implementation requires 22GE, while the 88×S-box requires at least 200GE. Therefore, in the design of lightweight cryptographic algorithms, 44×S-box is usually used instead of 88×S-box. Although hardware implementation efficiency is the first estimate of lightweight cryptographic algorithms, software application efficiency is also an aspect of its evaluation. In some environments, algorithm software applications are also required. When evaluating the effectiveness of software applications, we usually use C programming to implement and then test the algorithm to process different lengths of information on different platforms and finally calculate the time required for its efficiency [31].

2.4 Experiment

2.4.1 Geometric modeling of the manipulator

This article uses ADAMS simulation analysis software for experimental analysis. It is not only used for complex 3D modeling work, but also takes a long time to complete, and it cannot effectively ensure the dimensional accuracy and precision of the assembly position of the 3D model. Therefore, the modeling of the multifunctional side-by-side garbage truck involved in this article uses Solidworks software, and the embedded original geometric model is converted and imported into the ADAMS/View environment, constraints and loads are added, and simulation analysis is performed.

My country's "motor vehicle lane width design standard" clearly stipulates that the width of each lane in a multi-lane highway (above level three) should be designed

within the range of 3.5m–3.75m. For the diversion lanes of urban intersections, the width of each lane is designed to be 2.3 to 2.5m; for general urban roads, the width of each lane is designed to be 1.5m. The manipulator designed in this model has a limit length of 3m in the Y-direction rail box-type boom, plus the length of the manipulator's gripper itself is 0.2m, so the simulation parameters for the Y-direction rail box-type boom in this paper are designed to be 2.8m, 2.4m, and 1.4m. According to the survey, there are two height differences between the discharge position of urban garbage bins in my country and the ground position, which are 0.0 m and 0.1 m, respectively. In this paper, two forms of step heights of 0.0 m and 0.1 m are selected.

In summary, the daily actual operation of the side-mounted garbage truck multifunctional manipulator mainly includes the typical operating conditions shown in Table 1.

3 Results and discussion

3.1 Geometric modeling of the manipulator

In order to accurately analyze the dynamic characteristics of the operator, after completing the 3D model of the multifunctional trash can operator, input it into ADAMS, and use the constraint module in the ADAMS simulation software to complete the application of mechanical power constraints to restrict the main operator relative movement. According to the characteristics of the model course in this document, the model mainly has the following four types of constraints.

1) Constraints of commonly used motion pairs, including rotating pairs, sliding pairs, gear pairs, and fixed pairs;
2) The restriction of the designated direction, that is, the restriction is the designated moving direction of each part of the operator during the waste collection process, such as the extension direction or the contraction of the extension arm.
3) The contact restriction mainly refers to the restriction of the contact process of the cam mechanism between the cam and the guide rod by the two components.
4) Movement restriction mainly refers to the restriction of elements in the process of defining the movement trajectory, for example: defining specific elements for monitoring specific step functions.
5) The numerical parameter values of the specific model are shown in Table 2 and Fig. 2.

Table 1 Main three operating conditions settings

Working condition	Y item rail arm length	Quality of trash can	Step height
Working condition 1	1400	50	
		100	0
		150	100
Working condition 2	2100	50	
		100	0
		150	100
Working condition 3	2300	50	
		100	0
		150	100

Table 2 Parameter values set by the model

Contact	Stiffness coefficient	Elasticity index	Coefficient of static friction	Dynamic friction coefficient
CONTACT_5	1.00E+10	2.2	0.5	0.3
CONTACT_9	1.00E+10	2.2	0.5	0.3
CONTACT_13	1.00E+07	1.5	0.6	0.5
CONTACT_15	1.00E+08	2.2	0.3	0.1

In the impact model of ADAMS software, four main contact parameters of the model are defined, namely stiffness coefficient, tensile strength index, static friction coefficient, and dynamic friction coefficient. Different models and motions of machinery correspond to different parameters related to contact constraints, which must be adjusted according to the actual state of the machinery. The parameter values defined in the model in this article are shown in Table 3-1, and other parameters adopt the default values recommended by ADAMS software. Among the parameters defined by the model, the choice of stiffness factor has an important influence on the operation of the operator system. If the finger cuts into the trash can during the entire operator simulation calculation process, it means that the stiffness coefficient within the contact limit of the model is too small. If the operator vibrates or bounces violently, it means that the stiffness factor in the model contact limit is set to "too large."

3.2 Driving and external load

After completing the definition of the kinematics pair and the contact constraints between the components in the entire calculation model, in order to simulate and analyze the kinematics and dynamics of the entire system under the action of related external forces, this paper uses a side trash can. Specific external force or motion will be applied to the operating system calculation model. Therefore, ADAMS software provides many different types of external force and torque functions to meet the needs of complex mechanical system dynamic simulation. It can be seen from the multifunctional structure of the side trash can, and the movement track of the operator handle that the

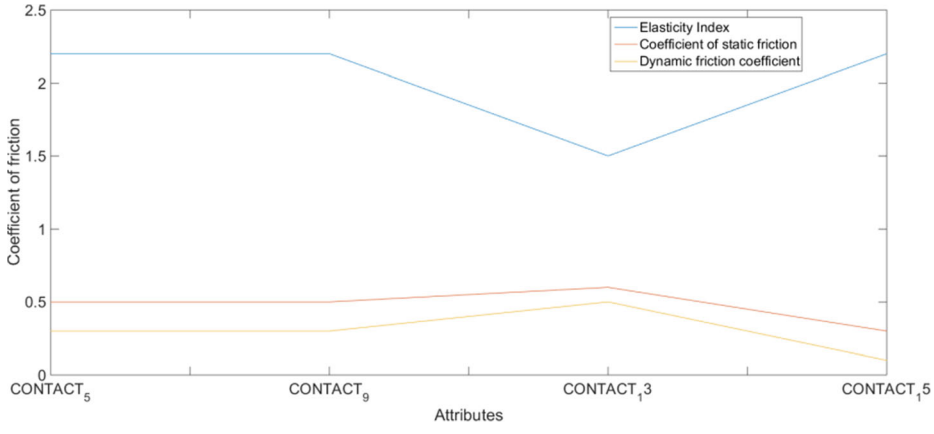

Fig. 2 Parameter values set by the model

Table 3 Usage of trash bins with different shapes

Shape	Market share (%)	Volume
Round	22.4	50, 100, 120
Rectangle	65.1	50, 100, 120, 240
Other shapes	11.5	0, 80, 100, 200

operator handle must complete four actions: quasi-trash can, approaching the trash can, tightening the trash can, and lifting the trash can. These four operations must be performed by the force generated by the expansion and contraction of the X-direction hydraulic cylinder, the Y-direction hydraulic cylinder, the Z-direction hydraulic cylinder, and the symmeStrical hydraulic clamping cylinder. Perform operations, step mode, if mode and many other internal drives functions, because the movement rules of the multifunctional operator of the side truck are complicated, and the movement space of the operator's handle completely depends on the movement path of each hydraulic cylinder during the entire process of waste collection. Combining the operator's law of motion and improving the reliability of dynamic analysis, the operator's motion design has the functions of X-direction hydraulic cylinders, Y-direction hydraulic cylinders, Z-direction hydraulic cylinders, and symmetric b-cylinders with ST-b all-wheel drive.

The external load of the side-mounted garbage truck multifunctional manipulator model is mainly the weight of the garbage can, so the corresponding changes are made according to the different masses of the garbage can during the simulation calculation. In this paper, the quality of the trash can is edited by modifying the material properties of the trash can part, and the quality setting is completed.

Because the relative position of the garbage can and the garbage truck is random, this requires the garbage truck to move in the X, Y, and Z directions during daily operations. The X direction is the running direction of the vehicle, which is mainly determined by the gripping width of the manipulator. The Y direction is the lateral direction, and the movement of Y mainly controls the lateral distance between the garbage can and the garbage truck, which is completed by the telescopic boom. The Z direction is the height direction, and the collection operation of the trash can is realized by rotating the lifting height of the Z-direction guide rail. In order to meet the needs of the real working environment, the side-mounted garbage truck multifunctional manipulator involved in this article should meet the simulation of a variety of typical working conditions in the garbage collection process, through the quality of the garbage can, the length of the Y-directional rail box-type boom, and the road shoulder The simulation of the manipulator is realized only at the height of the steps. As shown in Table 3 and Fig. 3.

According to the survey of the status quo of domestic garbage bins for urban residents in my country (Table 3), the shape of the garbage bins is mainly rectangular, circular, and other shapes. The volume of trash cans is generally concentrated in 50L, 100L, 120L, and 240L. Because rectangular trash cans are widely used, this article mainly analyzes four rectangular trash cans with different volumes. The specific models and specifications are shown in Table 4 and Fig. 4.

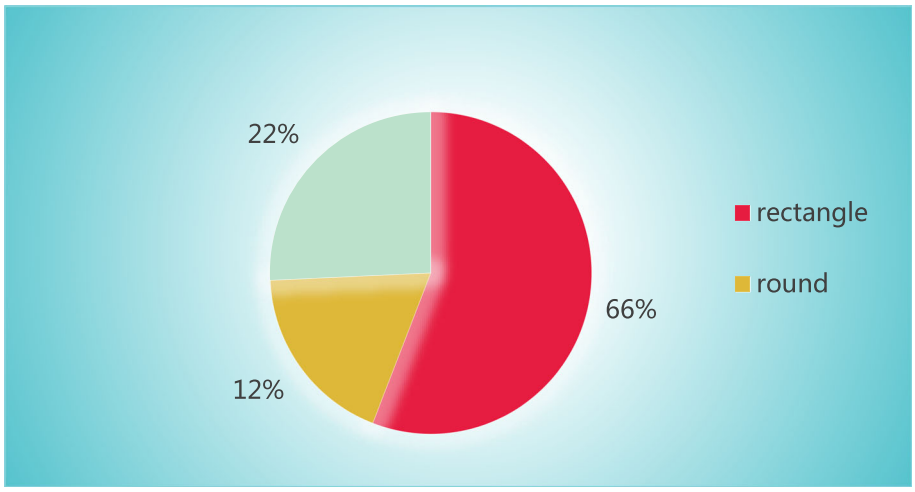

Fig. 3 Usage of trash cans with different shapes

3.3 Simulation analysis of typical working conditions

In order to correctly simulate the effects of typical working conditions, this article must accurately describe the laws of motion of the mechanism and drive components. Table 5 shows the working conditions of the hydraulic cylinder in a specific operating procedure. The entire movement process requires the waste bins to be aligned, the waste containers to be tightened, and the waste containers to be lifted. In order to improve work efficiency, the operator needs two or three hydraulic cylinders to operate simultaneously during the entire waste collection process, and the overall effect of the composite material takes 8-11s.

This article uses typical operating condition 1 as an example for simulation analysis. In typical operating condition 1, the Y-directional rail arm of the side-mounted garbage truck multifunctional manipulator is 1.4 m long, that is, the third arm of the manipulator is fully extended, the height difference between the trash can and the ground is 0.1 m, and the mass of the trash can is set as 50, 100, and 150kg. The STEP functions driven by the four hydraulic cylinders in the software are specifically set. It is shown in Table 6.

For three different quality trash cans, the manipulator completes the grabbing of the trash can before 3.5s. Among them, the support reaction curve at the X and Y guide rail interface basically keeps coincident. During the period of 3.5s to 5.5s, the bearing reaction force curve increased to a certain extent and showed the largest bearing reaction force. This shows that at a certain time from 3.5s to 5.5s, the Y-direction rail box robot arm has reached 1400mm in length and started to move in the Z direction, and the trash can is just off the ground; after 5.5s, with the Z direction when moving, the

Table 4 Specific models and specifications of trash bins with different volumes

Model	Volume	Specification	Total mass
ST-50	50	470 × 430 × 595	32
ST-100	100	550 × 480 × 810	64
ST-120	120	540 × 480 × 950	76.8
ST-240	240	740 × 600 × 1000	153.6

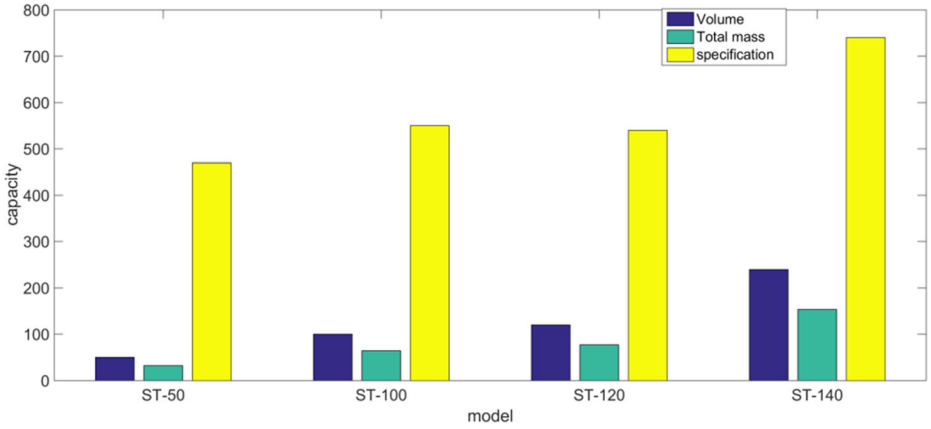

Fig. 4 Specific models and specifications of trash bins with different volumes

Y-direction guide rail begins to shrink, and the reaction force curve of the support decreases to a certain extent, and the change rule of the curve conforms to the actual situation. The maximum bearing reaction force at the X, Y guide rail interface is shown Table 7 and Figs. 5 and 6.

3.4 Optimization analysis of manipulator

In the working process of the side-mounted garbage truck manipulator, the trash can gripper at the front end and the joint arm of the axial manipulator are the main structures for carrying capacity. After repeated extension, pitch, and overload conditions, it is easy to make the front end of the manipulator the structure and arm have fatigue deformation and stress overload, and even break. Therefore, the rigidity and strength of the gripper at the front end of the garbage truck manipulator and the extended arm structure determine the reliability, service life, and performance of the garbage truck. Therefore, in the early stage of structural design, it is necessary to perform simulation analysis on the mechanical arm of the side-mounted garbage truck, mainly for the front-end gripper of the manipulator and the relevant force analysis and verification of each arm. Combined with the static analysis results of the finite element analysis, the overall structure is optimized and the structure is rationally designed to ensure the stability and reliability of the manipulator in the actual use.

Table 5 Working hours of hydraulic cylinders in garbage collection process

Robot operation process	X direction hydraulic cylinder	Y direction hydraulic cylinder	Z direction hydraulic cylinder	Clamping hydraulic cylinder to work
Trash can alignment	1.5–2.5s			
Trash can approaching		1.5–2.1s		
Trash can clamping				1.5–2.5s
Trash can rise			2.2s	
Robot recycling		1.9s		

Table 6 Specific settings of STEP function driven by each hydraulic cylinder

Hydraulic cylinder direction	STEP function settings
X direction hydraulic cylinder	STEP (time , 0, 0, 1.5, −0.6) + STEP (time, 5.5, 0, 7.5, 0.6)
Y direction hydraulic cylinder	STEP (time,0, 0, 1.5, −1.4) + STEP (time 5.5, 0, 7.5, 1.4)
Z direction hydraulic cylinder	STEP (time,3.6 ,0, 5.5, −0.2)
Step up hydraulic cylinder	STEP (time, 1.5, 0, 3.5, −0.139)

In this regard, this article uses the workbench finite element simulation software to analyze the side-mounted mechanical arm, study the stress changes of the front-end gripper and arm of the manipulator under various working conditions, and detect the effectiveness of its structural design. The following structural optimization of the car manipulator provides a certain basis.

The form of the load is mainly concentrated force at the gripper and distributed load at the joint arm. The applied form is determined according to the actual working conditions of the manipulator. In the load application process, in order to avoid the concentration of stress caused by a single load concentrated on a certain node, it is necessary to calculate the equivalent load applied to the contact surface of the manipulator. The specific operation method is as follows: (1) In the load application of each arm, its own weight is applied in the form of acceleration of gravity, and each arm uses the same application method. (2) The application of the gravity load of the trash can is calculated according to the horizontal and longitudinal distance from the position of the center of gravity of the trash can to the grip of the manipulator. In addition, the gripping force of the grip is applied to each grip in a uniformly distributed load (hand). (3) At each restraint, the restraining force at the junction and support is applied to the corresponding position. In the load application, the load applied by the garbage truck manipulator is shown in Table 8.

4 Discussion

In the actual work process of the garbage truck manipulator, various components need to be integrated into a whole structure through certain connections, such as welding, junction, and riveting. But this article still has some shortcomings. For example, this article is only to simulate and optimize the manipulator through simulation, so it may not be consistent with the actual situation because the actual movement is affected by external factors. It may cause the standard data to not adapt to the real work environment very well. These connections can be effectively integrated with the help of workbench software. The actual operation of the garbage truck has carried out the preliminary integration of the various connections of the manipulator. In the normal operation of the mechanical arm, the force transmission between each arm mainly borrows the slider body between the two, and the contact place is affected by friction.

Table 7 Comparison of front and rear reaction forces at the gripper interface of the manipulator

Bearing reaction force (N)	Trash can 50kg	Trash can 100kg	Trash can 150kg
Near the end hand interface	4421.2	5932.3	7463.2
Keep away from the end of the hand interface	−1812.2	−2910.9	−4031.8

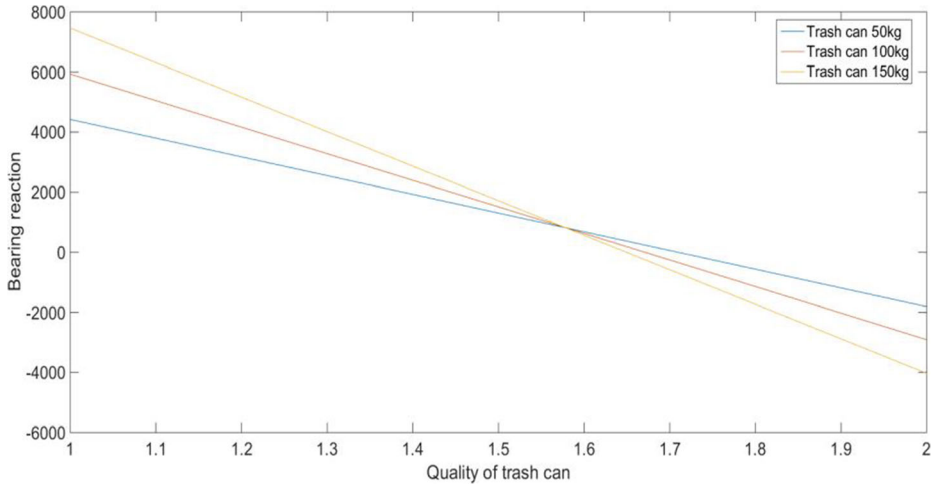

Fig. 5 Comparison of front and rear reaction forces at the gripper interface of the manipulator

However, in the finite element force analysis, due to the coefficient of friction between each arm, it is relatively small and belongs to a small deflection range. Therefore, a combination of degrees of freedom technology can be used to simulate the slider connection between each mobile phone. In addition, the load borne by the multifunctional manipulator in actual work mainly includes the clamping force of the trash can gripper at the front end of the manipulator, the gravity of the trash can itself, and the weight of each joint arm.

5 Conclusions

Based on the actual application of the garbage truck, this paper studies the intelligent kinematic analysis of the multi-functional manipulator in actual operation and the finite element analysis of the force of the manipulator. On the basis of studying the structure of various garbage trucks at home and abroad through the Internet of Things,

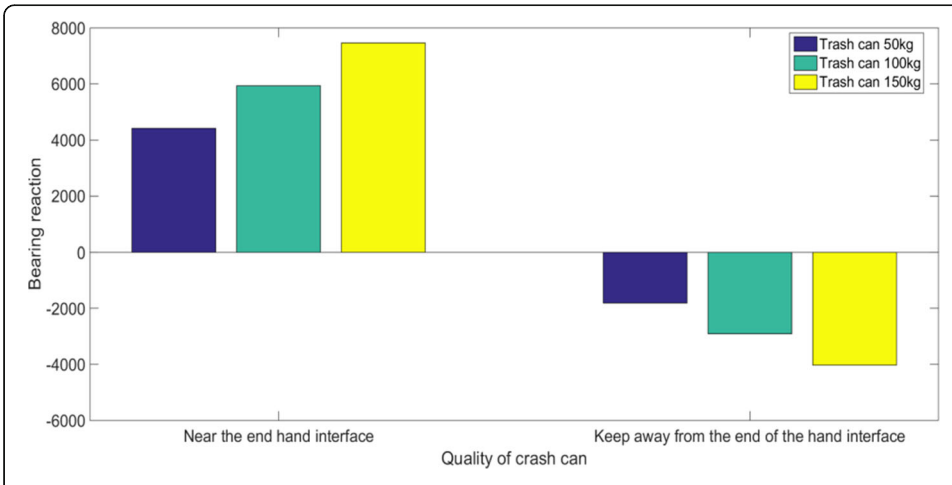

Fig. 6 Comparison of front and rear reaction forces at the gripper interface of the manipulator

Table 8 Load size of manipulator

Structure name	Size/N	Types
Trash can weight	1400	Concentrated load
Weight of fixed arm	550	Acceleration of gravity
The weight of the second arm	380	Acceleration of gravity
Forearm weight	300	Acceleration of gravity
Trash can handle weight	370	Acceleration of gravity

the existing garbage truck manipulators in my country are summarized and compared, and the characteristics of the movement of the garbage truck manipulators are analyzed. Based on the current development status and future development trends of garbage truck manipulators in my country, several aspects such as improving the strength of manipulators, lightweight, and reliable performance have been studied. Expectations for the future: In future work, we will improve the motion of the manipulator based on the actual application.

Abbreviations

ADAMS: Automatic Dynamic Analysis of Mechanical Systems; RFID: Radio frequency identification; GE: General electric; ASIC: Application Specific Integrated Circuit

Authors' contributions

Caiping Guo: Writing—editing. Daqing Li: data analysis. The author(s) read and approved the final manusccript.

Funding

The authors received no financial support for the research, authorship, and/or publication of this article.

Availability of data and materials

Data sharing does not apply to this article because no data set was generated or analyzed during the current research period.

Declarations

Ethics approval and consent to participate

This article is ethical, and this research has been agreed.

Consent for publication

The picture materials quoted in this article have no copyright requirements, and the source has been indicated.

Competing interests

The authors declare that they have no competing interests.

Author details

[1]School of Mechanical and Electrical Engineering, Jiaozuo University, Jiaozuo 454003, Henan, China. [2]School of Mechanical Engineering, Henan Institute of Engineering, Zhengzhou 451191, Henan, China.

Received: 10 April 2021 Accepted: 19 May 2021
Published online: 29 July 2021

References

1. M.E. Khanouche, Y. Amirat, A. Chibani, et al., Energy-centered and QoS-aware services selection for Internet of Things. IEEE Transact Automat Eng **13**(3), 1256–1269 (2016)
2. S. Mayer, J. Hodges, D. Yu, et al., An Open Semantic Framework for the Industrial Internet of Things. IEEE Intell Syst **32**(1), 96–101 (2017)
3. H. Sun, X. Wang, R. Buyya, et al., CloudEyes: Cloud-based malware detection with reversible sketch for resource-constrained internet of things (IoT) devices. Softw Pract Exp **47**(3), 421–441 (2017)
4. S.H.A.H.R. Chandra, W.A.N.G. Yafeng, Cloud Things Construction - the integration of Internet of things and cloud computing. Future Generation Comput Syst **56**(C), 684–700 (2016)
5. C. Chang, S.N. Srirama, R. Buyya, Mobile cloud business process management system for the internet of things: a survey. Acm Comput Surv **49**(4), 1–42 (2016)
6. M.D. Giudice, Discovering the Internet of Things (IoT) within the business process management. Bus Process Manage J **22**(2), 263–270 (2016)
7. M. Zhou, Y. Wang, Y. Liu, Z. Tian, An information-theoretic view of WLAN localization error bound in GPS-denied environment. IEEE Transact Vehicular Technol **68**(4), 4089–4093 (2019)

8. G. Yang, Q. Zhang, Y.-C. Liang, Cooperative ambient backscatter communications for green Internet-of-Things. IEEE Internet Things J **5**(2), 1116–1130 (2018)
9. R. Rajiv, R. Omer, N. Surya, et al., The next grand challenges: integrating the Internet of Things and data science. IEEE Cloud Comput **5**(3), 12–26 (2018)
10. J.C. Balda, A. Mantooth, R. Blum, et al., Cybersecurity and power electronics: addressing the security vulnerabilities of the Internet of Things. IEEE Pow Electron Mag **4**(4), 37–43 (2017)
11. M. Wolf, D. Serpanos, Safety and security in cyber-physical systems and Internet-of-Things systems. Proceed IEEE **106**(1), 9–20 (2017)
12. A. Tzounis, N. Katsoulas, T. Bartzanas, et al., Internet of Things in agriculture, recent advances and future challenges. Biosyst Eng **164**, 31–48 (2017)
13. G. Kecskemeti, G. Casale, D.N. Jha, et al., Modelling and simulation challenges in Internet of Things. IEEE Cloud Comput **4**(1), 62–69 (2017)
14. P.P. Jayaraman, X. Yang, A. Yavari, et al., Privacy preserving Internet of Things: from privacy techniques to a blueprint architecture and efficient implementation. Future Generation Comput Syst **76**(Nov.), 540–549 (2017)
15. C. Chang, S.N. Srirama, R. Buyya, Indie fog: an efficient fog-computing infrastructure for the Internet of Things. Computer **50**(9), 92–98 (2017)
16. N. Abuzainab, W. Saad, C.S. Hong, et al., Cognitive hierarchy theory for distributed resource allocation in the Internet of Things. IEEE Transact Wireless Commun **16**(12), 7687–7702 (2017)
17. I. Azimi, A.M. Rahmani, P. Liljeberg, et al., Internet of things for remote elderly monitoring: a study from user-centered perspective. J Ambient Intell Humanized Comput **8**(2), 273–289 (2017)
18. C. Aranzazu-Suescun, M. Cardei, Distributed algorithms for event reporting in mobile-sink WSNs for Internet of Things. Tsinghua ence Technol **22**(4), 413–426 (2017)
19. M. Zhou, Y. Li, M.J. Tahir, X. Geng, Y. Wang, W. He, Integrated statistical test of signal distributions and access point contributions for Wi-Fi indoor localization. IEEE Transact Vehicular Technol (2021). https://doi.org/10.1109/TVT.2021.3076269
20. I. Yaqoob, E. Ahmed, M.H.U. Rehman, et al., The rise of ransomware and emerging security challenges in the Internet of Things. Comput Netw **129P2**(DEC.24);129:444–458 (2017). https://doi.org/10.1016/j.comnet.2017.09.003
21. X. Lin, J. Bergman, F. Gunnarsson, et al., Positioning for the Internet of Things: a 3GPP perspective. IEEE Commun Mag **55**(12), 179–185 (2017)
22. Z. Ling, J. Luo, Y. Xu, et al., Security vulnerabilities of Internet of Things: a case study of the Smart Plug System. IEEE Internet Things J **4**(6), 1899–1909 (2017)
23. A. Rizzardi, S. Sicari, D. Miorandi, et al., AUPS: an Open Source AUthenticated Publish/Subscribe system for the Internet of Things. Inf Syst **62**(dec.), 29–41 (2016)
24. J. Yu, M. Kim, H.C. Bang, et al., IoT as an applications: cloud-based building management systems for the internet of things. Multimedia Tools Appl **75**(22), 14583–14596 (2016)
25. O. Iova, P. Picco, T. Istomin, et al., RPL, the Routing Standard for the Internet of Things. Or Is It? IEEE Commun Mag **54**(12), 16–22 (2016)
26. T. Xu, I. Darwazeh, Non-orthogonal narrowband Internet of Things: a design for saving bandwidth and doubling the number of connected devices. IEEE Internet Things J **5**(3), 2120–2129 (2018)
27. V.H. Le, J. Den Hartog, N. Zannone, Security and privacy for innovative automotive applications: a survey. Comput Commun **132**(NOV.), 17–41 (2018)
28. L. Li, G. Ren, Y. Liu, et al., Secure DHCPv6 mechanism for DHCPv6 security and privacy protection. Tsinghua ence Technol **23**(001), 13–21 (2018)
29. Z.P. Zhang, M. Fu, X.Y. Feng, A lightweight dynamic enforcement of privacy protection for android. J Comput Technol **34**(4), 901–923 (2019)
30. L. Hongwei, L. Rongxing, M. Jelena, et al., Security and privacy of connected vehicular cloud computing. IEEE Netw **32**(3), 4–6 (2018)
31. N. Kaaniche, M. Laurent, Data security and privacy preservation in cloud storage environments based on cryptographic mechanisms. Comput Commun **111**(oct.1), 120–141 (2017)

Publisher's Note